

Numerical Simulation of Nonswirling and Swirling Annular Liquid Jets

Stephen G. Chuech*

Delavan, Inc., West Des Moines, Iowa 50265

A numerical simulation method is described for analyzing the fluid dynamics of nonswirling and swirling annular liquid jets. In the present theoretical study, a general mathematics model for simulating these two types of annular film jets has been established using a curvilinear coordinate system conforming to the film boundaries. The study involves the derivation of governing equations, numerical solutions for annular film flow structure of both nonswirling and swirling cases, and model validation with available measurements. The solutions of flow structure consist of jet velocity, film thickness, and jet trajectory. The present model can predict the "transition" phenomenon of jet-shape formation from nonswirling "bell" to swirling "hollow cone." In verification studies, first the model is validated against other measurements and analyses of nonswirling bell-like jets. The second case includes a validation study on spray angle of swirling conical sprays and a comparison of fuel spray configuration of a pressure atomizer. The assessment results are encouraging and indicate a good capability of the current model.

Nomenclature

A	= area
C	= mass flux
D	= diameter of annular film
F	= friction force
f	= friction coefficient functions
G	= gravity term of momentum equation
g	= gravity acceleration
L	= bell length
m	= mass flow rate
p	= static pressure
R	= second principal radius of curved surface
Re	= Reynolds number
r	= first principal radius of curved surface or radial distance in the y direction
S	= viscous term of momentum equation
s	= streamwise distance in the ξ direction
u	= streamwise velocity in the ξ direction
V	= control volume
v	= normal velocity in the η direction
w	= swirling velocity
X	= axial coordinate in cylindrical system
Y	= radial coordinate in cylindrical system
δ	= film thickness
ζ	= tangential coordinate in curvilinear system
η	= normal coordinate in curvilinear system
θ	= angle between ξ coordinate and X coordinate
μ	= viscosity
ξ	= streamwise coordinate in curvilinear system
ρ	= density
σ	= surface tension
ϕ	= angle of curve Δs

Subscripts

c	= index of the film cross section
f	= liquid film
g	= gas phase

s	= index of the film circumference
ζ	= tangential component in curvilinear system
η	= normal component in curvilinear system
ξ	= axial component in curvilinear system
0	= initial or jet exit condition

Introduction

A NONSWIRLING annular liquid jet is a liquid film issuing from an annular orifice and is also called a "liquid curtain."¹⁻³ When the liquid curtain velocity is low, surface tension acting on the circumferential surfaces causes the film to coalesce after a short distance and then to continue with a full "solid" cross section. This type of jet has been of academic and practical interest since the 19th century. Boussinesq⁴ first proposed a mathematical model for water bells. Then the concept of water bells was used to determine the surface tension of water, mercury, and other liquids. Later, more studies of water bells were done by many researchers,⁵⁻⁹ involving the effects of gravity, surface tension, and pressure difference between the inside and outside of the bell.

Recently, attention on this subject has grown due to the concept of utilizing a liquid annular jet as confined chemical reactors¹ and inertial confinement laser fusion reactors.² The main purpose of using annular liquid jets or liquid curtains for these chemical reactors is to alleviate problems associated with toxic reaction, protection system, and pollution control. The chemical reactors based on annular liquid jets have been described and mathematically modeled by Hovingh,¹⁰ Hoffman et al.,¹¹ and Ramos.^{1,2} However, these Lagrangian models^{1,2,10,11} still used the equations similar to those for water bells originally derived by Boussinesq.⁴

Swirling Jet

For a swirling annular liquid jet, there exists an additional centrifugal force to interact with surface tension, pressure, and gravity. When the swirling velocity is increased, the centrifugal force gradually becomes dominant, and then the liquid curtain opens up with an angle. This is known as the "hollow cone" in spray flows. The hollow cone has been used for spray and atomization processes in combustion systems, agriculture and aerosol production, and others. In the case of a gas turbine, such a hollow conical film is produced by injection of the liquid fuel and disintegrates into ligaments and droplets in the combustion chamber. Therefore, the hollow cone film has an important impact on the spray characteris-

Presented as Paper 92-0464 at the AIAA 30th Aerospace Sciences Meeting, Reno, NV, Jan. 6-9, 1992; received Jan. 13, 1992; revision received Sept. 9, 1992; accepted for publication Sept. 14, 1992. Copyright © 1992 by the American Institute of Aeronautics and Astronautics, Inc. All rights reserved.

*Senior Research Engineer, Gas Turbines Division; currently Senior Research Engineer, Taiwan Aerospace Corporation, Taipei, Taiwan. Member AIAA.

tics,¹² such as drop formation rate, drop velocity, drop size and spatial distribution, and spray angle, etc.

Over the past decade, although many computational fluid dynamics (CFD) tools have been useful during the combustor design and development phases, their capability to provide accurate predictions is strongly dependent on the empirical spray characteristics as input conditions for a given combustion system.^{13,14} In general, the applicability of experimental information describing spray characteristics for a certain design is obviously questionable for others.

Furthermore, for predicting spray combustion in gas turbines, currently existing CFD codes and models all neglect the presence of the hollow cone film and assume instantaneous atomization at the nozzle exit. Past studies^{13,14} indicate that predicted results are very sensitive to the assumed atomization characteristics. To remove these drawbacks, an analytical model to simulate the hollow cone phenomenon is needed to provide a fundamental basis for spray characteristics predictions.

General Remarks

Both nonswirling and swirling annular liquid jets are of vital importance to practical applications for liquid chemical reaction and fuel combustion. In the present study, a general mathematical model has been developed to simulate nonswirling and swirling annular liquid jets. The fundamental equations governing the liquid film flow, including a set of continuity and three momentum equations, were derived in a curvilinear coordinate system. These equations were integrated over a discretized control volume and numerically solved for liquid film trajectory, thickness, and velocity components. The analysis involved swirling hollow cone cases, as well as liquid curtain problems in which the swirling velocity vanished. The present model involves the effects of gravity, surface tension, pressure difference across the film, and friction effects on the film surface. For testing the model, the present predictions were compared with available measurements.

Mathematical Model

In the present model, it is assumed that a swirling film with an angle θ , shown in Fig. 1, is a one-dimensional, steady-state flow with no pressure gradient in the ξ (streamwise) and ζ (circumferential or tangential) directions. Viscous forces within the liquid are neglected, but the viscous friction forces at the gas-liquid interfaces are accounted for. Past studies on the general conservation form of equations in curvilinear coordinates have been reported in the literature.^{15,16} In the present work, the scalar equations are obtained by taking the inner product of the conservation form with unit vectors of curvilinear coordinates. Then, using the transformation law

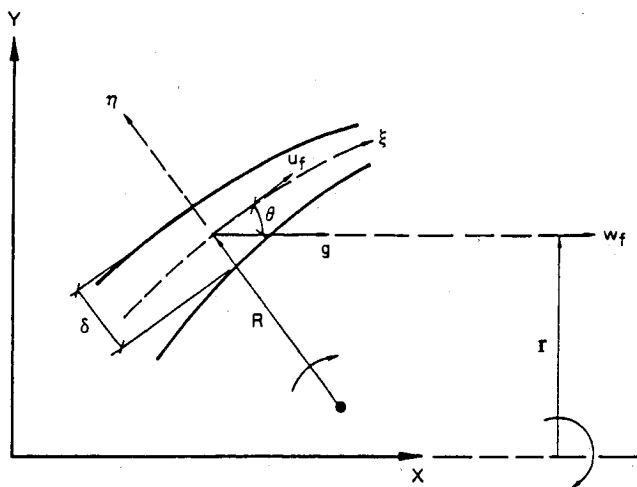


Fig. 1 Annular liquid film jet in the cylindrical coordinate and curvilinear coordinate systems.

for the covariant and the contravariant unit vectors, as well as aforementioned assumptions, the simplified equations governing the annular liquid flow in a curvilinear coordinate system can be formulated, including a set of continuity and three momentum equations:

Continuity:

$$\partial_{\xi}(C_{\xi}) = 0 \quad (1)$$

Streamwise momentum:

$$\partial_{\xi}(C_{\xi}u_f) - C_{\zeta}w_f \sin\theta/r = S_{\xi} + G_{\xi} \quad (2)$$

Normal momentum:

$$C_{\xi}u_f \partial_{\xi}(\theta) - C_{\zeta}w_f \cos\theta/r = -\partial_{\eta}(p_f) + G_{\eta} \quad (3)$$

Tangential momentum:

$$\partial_{\xi}(C_{\xi}w_f) + C_{\zeta}u_f \sin\theta/r = S_{\zeta} \quad (4)$$

where ∂_{ξ} , ∂_{η} , and ∂_{ζ} are partial differential operators with respect to ξ , η , and ζ . It would be desirable to solve for the liquid streamwise velocity u_f and swirling velocity w_f simultaneously by coupling Eqs. (2) and (4) via the centrifugal and Coriolis forces.

The viscous terms S_{ξ} and S_{ζ} are accounted for through the interfacial friction forces on both sides of the film. The general forms of the friction forces are

$$F_{\xi} = 0.5 \rho_g f_{\xi} (u_g - u_f) |u_g - u_f| \quad (5)$$

$$F_{\zeta} = 0.5 \rho_g f_{\zeta} (w_g - w_f) |w_g - w_f|$$

According to Rizk and Lefebvre,¹⁷ the interfacial friction factors are given by

$$f_{\xi} = 0.79(1 + 150\delta/r)(Re_{\xi})^{-0.25} \quad (6)$$

$$f_{\zeta} = 0.79(1 + 150\delta/r)(Re_{\zeta})^{-0.25}$$

where the Reynolds numbers $Re_{\xi} = \rho_g D |u_g - u_f|/\mu_g$ and $Re_{\zeta} = \rho_g D |w_g - w_f|/\mu_g$.

When the normal η -direction momentum equation, Eq. (3), is in an integrated form, the pressure term becomes the pressure difference Δp_f between the outer and inner surfaces, which can be related to capillary pressure¹⁸ and gas pressure difference Δp_g and is given as

$$\Delta p_f = \Delta p_g - 2\sigma(\cos\theta/r \pm 1/R) \quad (7)$$

The plus sign in front of $1/R$ is applied for the negative $d\theta/d\xi$ case, and the minus sign is for the positive $d\theta/d\xi$ case. By substituting Eq. (7), the normal momentum equation, Eq. (3), becomes

$$\begin{aligned} \rho_f A_c u_f^2 (\theta - \theta^*) - \rho_f V w_f^2 \cos\theta/r \\ = \Delta p A_s - 2\sigma(\cos\theta/r \pm 1/R) A_s - \rho_f g V \sin\theta \end{aligned} \quad (8)$$

where the control volume $V = r\delta\Delta s$, the cross-sectional area of the control volume $A_c = r\delta$, and the surface area of the control volume $A_s = r\Delta s$. Note that the superscript * represents the value of the previous calculation step in space.

In the present formulation of the surface conforming system, the normal velocity to the surface is zero, $v_f = 0$. Instead, the film angle and thickness become unknown. Equation (8) is used to calculate the film angle θ along the X axis, whereas the film thickness δ is solved through the continuity equation, Eq. (1). Furthermore, the other variables for the film location and shape (i.e., r , R , and X) can be determined from geometric relationship of film trajectory. Figure 2 illustrates the geometric relationship for a moving film in the cylindrical system.

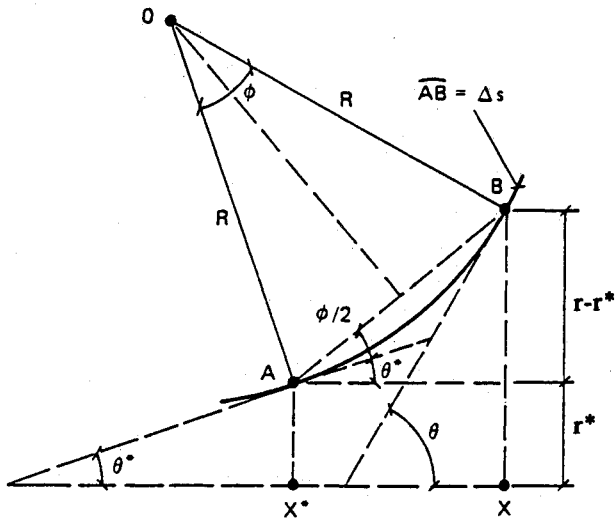


Fig. 2 Illustration of geometric relationships for a moving film in the cylindrical system.

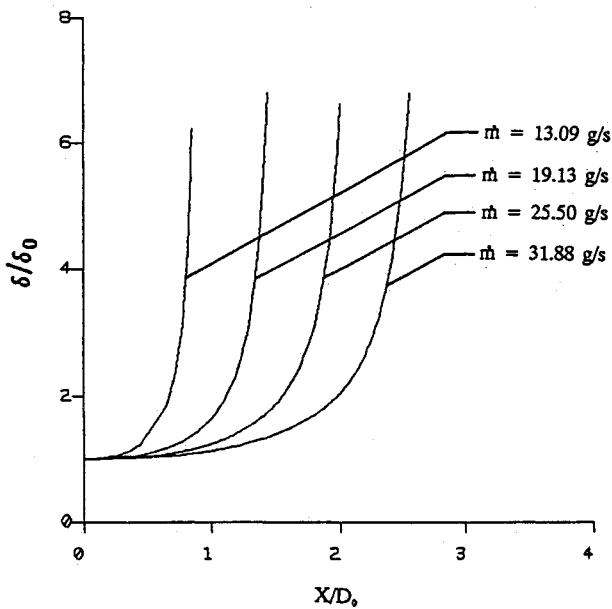


Fig. 3 Axial variations of film thickness for nonswirling annular water jets with different flow rates.

The expression for the two principal radii of curvature, r and R , can be easily obtained (where $\phi = \theta - \theta^*$):

$$R = \Delta s / |\phi| \quad (9)$$

$$r = r^* + |2R \sin(\phi/2)| \sin(\theta^* + \phi/2) \quad (10)$$

Also, space marching in the axial direction of the cylindrical system is given as

$$X = X^* + |2R \sin(\phi/2)| \cos(\theta^* + \phi/2) \quad (11)$$

In the present model, when the swirling velocity of the liquid film is set to zero, the entire model is simplified and becomes applicable for the nonswirling liquid curtain case.

Results and Discussion

Nonswirling Jet

The measurements of Baird and Davidson⁹ have been selected to validate the present model. In the measurements, the mean diameter of the annular orifice was 1.241 cm, and the

initial film thickness was 0.029 cm. The annular water jet was injected vertically downward so that the initial film angle θ_0 is zero. Four test conditions were selected for the current analyses, and the flow rates were 13.09, 19.13, 25.50, and 31.88 g/s, respectively.

Predicted dimensionless variations of film thickness and streamwise velocity have been plotted as a function of axial distance in Figs. 3 and 4. The results show that, for a nonswirling annular jet, film thickness and streamwise velocity increase as the axial distance is increased. After emerging from

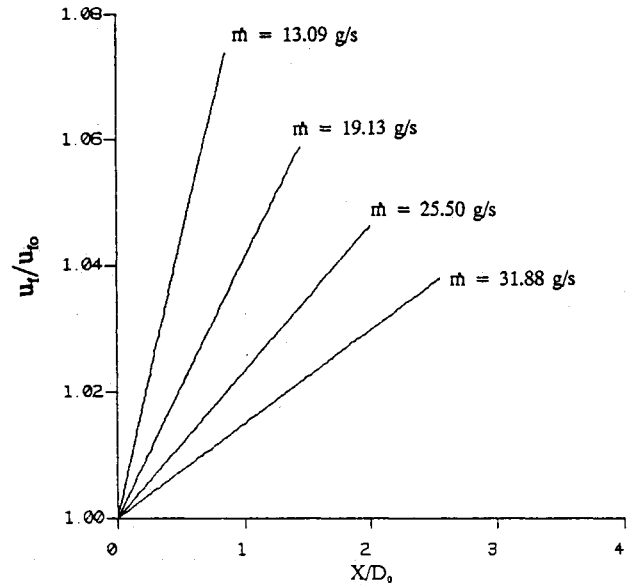


Fig. 4 Axial variations of streamwise velocity for nonswirling annular water jets with different flow rates.

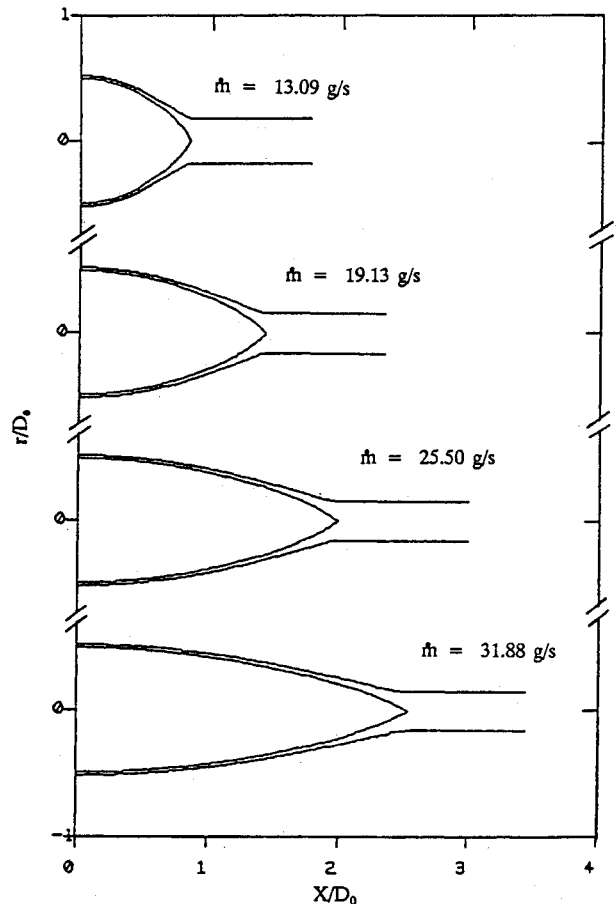


Fig. 5 Influence of liquid flow rate on the bell shapes of nonswirling annular jets.

the annular orifice, the annular film starts to contract toward the centerline due to surface tension. To satisfy the continuity equation, the film thickness and velocity have to be increased. Note that the water velocity is also accelerated by the gravity effect, but the surface tension effect is more dominant in the present case. Higher flow rate cases have smaller growth rates for film thickness and velocity, shown in Figs. 3 and 4. This is because higher flow conditions have higher inertia to overcome the contraction effect due to surface tension.

Figure 5 shows predicted shapes of the water bell jets at the same conditions as Figs. 3 and 4. The predicted film is curving toward the centerline and coalesces to become a cylindrical jet, as observed in past studies.⁵⁻⁹ From the bell shape variations, it can be seen that higher flow rate cases possess slower radius and angle variations, again due to higher inertia effects. The contraction effect on annular film decreases gradually with an

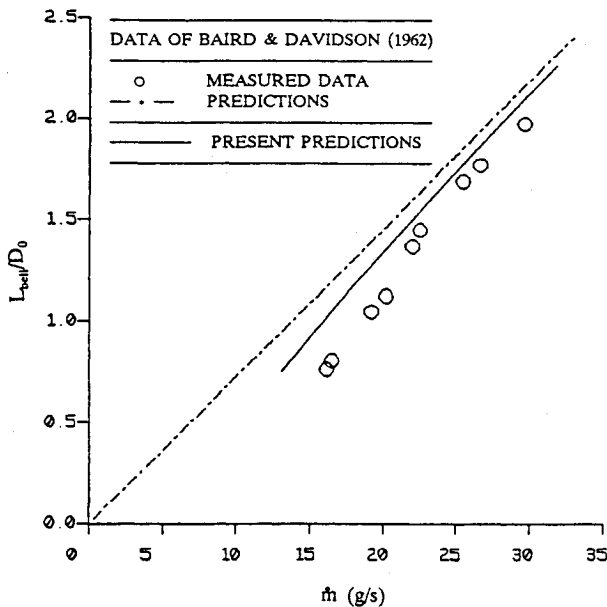


Fig. 6 Bell lengths of nonswirling annular jets with different flow rates.

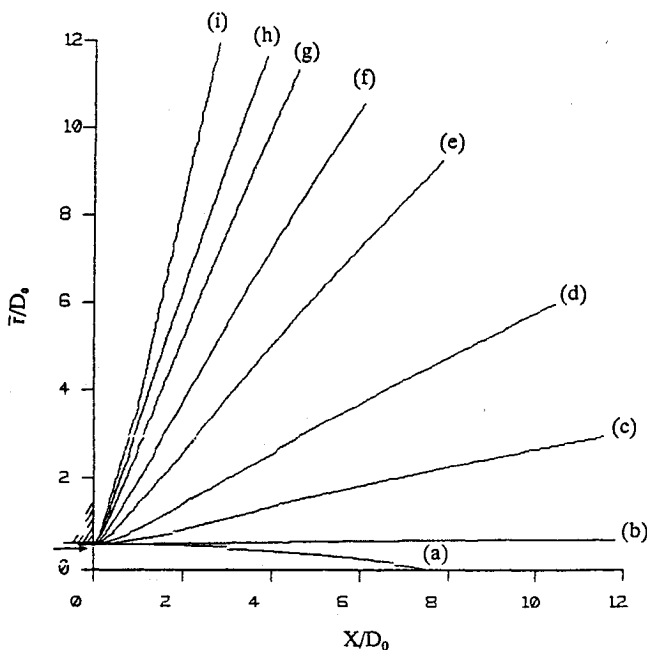


Fig. 7 Influence of swirler angle on the spray shape; swirler angle in degrees: a) 0, b) 1.5, c) 5, d) 10, e) 20, f) 30, g) 45, h) 60, and i) 80.

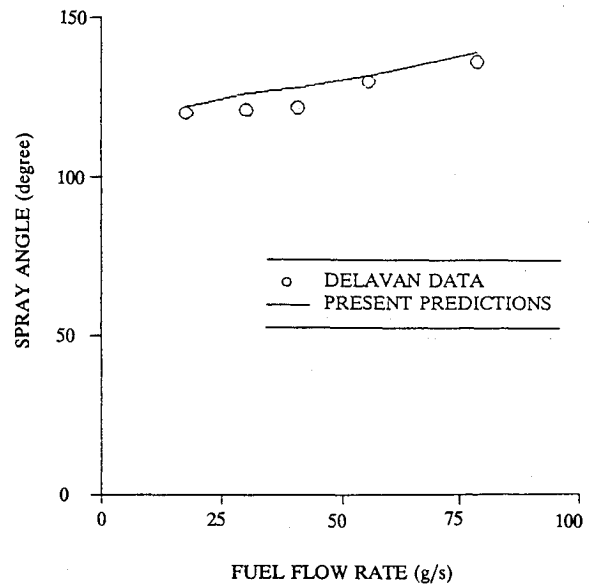


Fig. 8 Spray angles of swirling annular film jets with various flow rates.

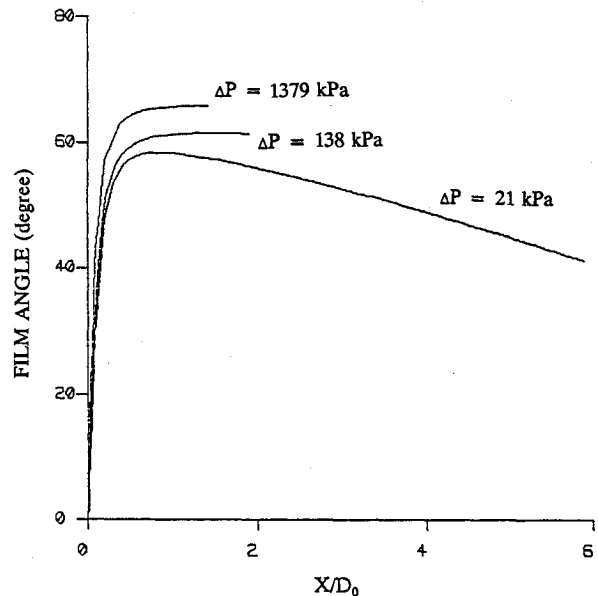


Fig. 9 Axial variations of film angle for swirling annular film jets at different operating conditions.

increase of the water flow rate. Figure 5 also indicates that the bell shape is elongated when the water flow rate is increased.

The bell length was defined as the distance below the orifice at which the external radius of the annular jet reached 0.2 cm.⁹ The predictions of bell length L_{bell} by Baird and Davidson⁹ can be expressed as

$$L_{bell} = 0.5D_0[\rho_f u_{f0}^2 \delta_0 (1 - r/r_0) / \sigma]^{0.5} \quad (12)$$

During the present study, Eq. (12) was also used to calculate the bell length, and the results were compared with predictions of the present model, as well as the measured data of Baird and Davidson.⁹ The comparison is presented in Fig. 6, in which dimensionless bell lengths of a nonswirling annular water jet are given as functions of flow rate. The present predictions agree well with measurements and exhibit a better agreement than the predictions of Baird and Davidson.⁹

Swirling Jet

To examine the effects of swirl on the shapes of the annular liquid film, the geometry of a Delavan nozzle with various

fuel-port angles was adopted for the analysis. The fuel-port angle is called "fuel swirler angle" in the present study. The fluid properties of tested fuel include density $\rho_f = 765 \text{ kg/m}^3$, viscosity $\mu_f = 9.2 \times 10^{-4} \text{ kg/m} \cdot \text{s}$, and surface tension $\sigma = 0.025 \text{ N/m}$. The fuel with a constant flow rate $\dot{m} = 0.01777 \text{ kg/s}$ was injected into still air. One quarter of the prefilmer width was taken as the initial film thickness $\delta_0 = 0.1524 \text{ mm}$. The initial film thickness was also assumed to be constant for different fuel swirler angles. Predicted film shapes for fuel swirler angles of 0–80 deg are shown in Fig. 7. The present predictions indicate that when swirl is added to the bell jet, the bell surfaces are pushed outward in the radial direction, and the film becomes a hollow cone. As the swirler angle is further increased, the conical film angle becomes larger. The present model can predict this "transition" phenomenon from the bell jet to conical film.

Spray angle is one of the important characteristics influencing combustion performance. It has a strong effect on ignition, stability limits, and exhaust smoke. To date, the spray

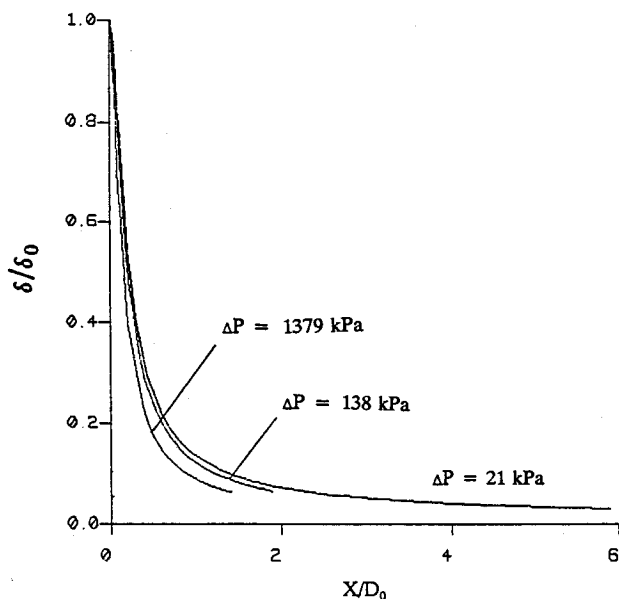


Fig. 10 Axial variations of film thickness for swirling annular film jets at different operating conditions.

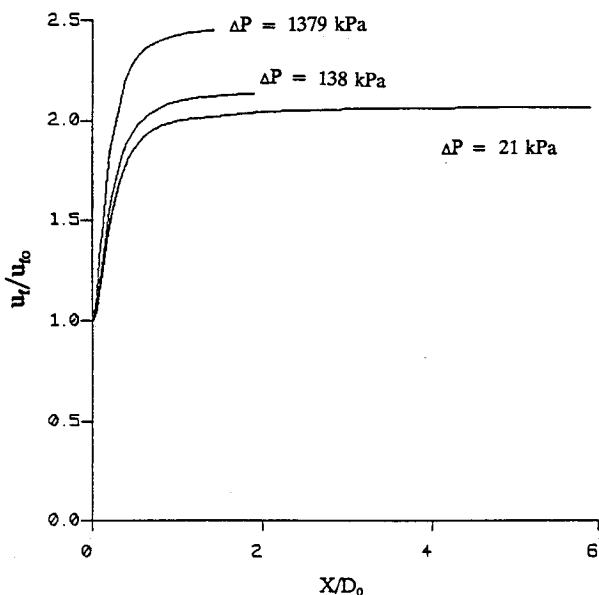


Fig. 11 Axial variations of streamwise velocity for swirling annular film jets at different operating conditions.

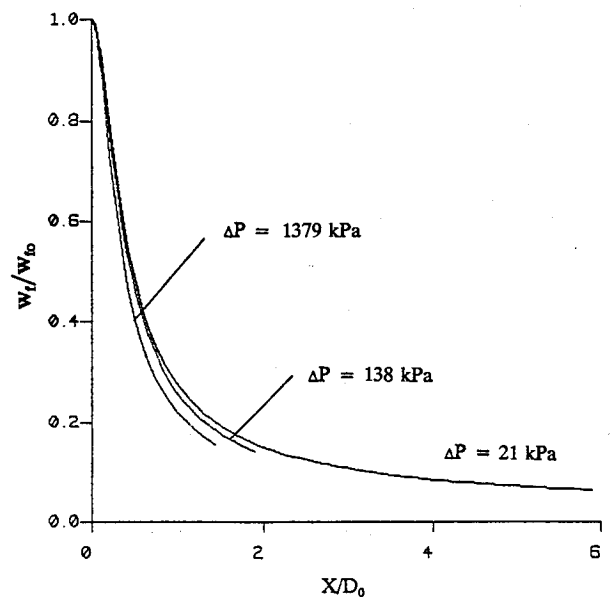


Fig. 12 Axial variations of swirling velocity for swirling annular film jets at different operating conditions.

angle has not yet been well defined.¹² In the present study, the maximum value of the film angle θ along the conic film trajectory is simply taken as the spray angle. As the flow rate increases, the conical spray should open to a larger spray angle. To verify the variation of spray angle with various fuel flow rates, the annular film issuing from a nozzle with a fuel swirler of 30 deg was analyzed at five test conditions (i.e., fuel flow rates $\dot{m} = 17.76, 30.24, 40.82, 55.69,$ and 79.13 g/s). In Fig. 8, the predicted spray angle and experimental data of these cases are plotted as a function of fuel flow rate. The predictions agree with measurements but overestimate them slightly.

To observe detailed structure of swirling annular jets, three additional cases at different fuel pressure conditions are analyzed and shown in Figs. 9–12. The variation of the film angle along the axial direction is shown in Fig. 9. The film angles at the two higher pressures initially increase faster than the lowest condition due to larger centrifugal effects. Although the film angles remain almost constant downstream, the spray shape at the lowest condition is curving downward to the centerline. For the lowest pressure, surface tension and gravity effects are more significant due to weaker inertia than the other two cases.

It is important to analyze the variation of the film thickness along the film trajectory for spray analysis because of its influence on drop size.¹⁹ Figure 10 presents the predictions of film thickness for various fuel pressures. An essential feature of mass conservation is that the film becomes thinner when the radius of the conical film is increased due to centrifugal force. In contrast to nonswirling cases, without centrifugal force, the film thickness of the nonswirling film increases due to the contraction effect of surface tension (see Figs. 3 and 5). Past studies¹⁹ indicate that the thinner a film thickness is, the smaller the spray drops will be. From Fig. 10, the film thickness at a higher pressure tends to decrease faster than in the lower pressure case. This trend implies that drops produced at higher fuel pressures could be smaller than those at lower conditions, as observed in past studies.¹⁹

Figures 11 and 12 present predictions of axial variations of streamwise and swirling velocities of the film flows. From these two figures, the film flow accelerates in the streamwise direction and decelerates in the swirling direction as the film moves downstream. The film velocity components are important because they have a critical impact on drop breakup and trajectory. The solutions of these velocity components need to be further validated against measurements.

Conclusions

The major conclusions of the present study are as follows:

1) A general mathematical model for nonswirling and swirling annular liquid jets was formulated and the nonlinear system of governing equations was solved for jet velocity, film thickness, and trajectory of both types of jets.

2) The present model can predict the "transition" phenomena of jet-shape formation from nonswirling bell to swirling hollow cone.

3) For nonswirling jets, the inertia effect due to increased flow rate reduces the contraction phenomenon and elongates the bell length. For swirling cases, the centrifugal force contributed by swirl effects interacts with surface tension to cause a variety of jet-shape formations.

4) For nonswirling annular jets, film thickness and streamwise velocity increase as the axial distance is increased due to the contraction effect of surface tension. However, for swirling cases, the streamwise velocity increases along the streamwise direction, but the film thickness decreases as a result of cone divergence due to centrifugal force.

5) To validate the model, our analyses were compared with measurements for nonswirling and swirling annular liquid jets. The comparisons showed good agreement between predictions and measurements for different fluids and a variety of test cases, including bell length, spray angle, and jet-shape transition. The comparison indicates that the current curvilinear coordinate formulation used for annular film dynamics can predict accurate results and can provide a good baseline for the further analysis of liquid curtain reactors and swirling conical sprays.

References

- ¹Ramos, J. I., "Analytical, Asymptotic and Numerical Studies of Liquid Curtains and Comparisons with Experimental Data," *Applied Mathematics Modelling*, Vol. 14, No. 4, April 1990, pp. 170-183.
- ²Ramos, J. I., "Liquid Curtains—I. Fluid Mechanics," *Chemical Engineering Science*, Vol. 43, No. 12, 1988, pp. 3171-3184.
- ³Kihm, K. D., and Chigier, N. A., "Experimental Investigations of Annular Liquid Curtains," *ASME Journal of Fluids Engineering*, Vol. 112, No. 3, March 1990, pp. 61-66.
- ⁴Boussinesq, M. J., "Theorie des experiences de Savart sur la frome que prend une veine liquide apres s'etre choquee contre un plan circulaire," *Comptes Rendus de l'Academie des Sciences*, Vol. 69, 1869, pp. 45-48 and pp. 128-131.
- ⁵Binnie, A. M., and Squire, H. B., "Liquid Jets of Annular Cross Section," *The Engineer*, Vol. 171, 1941, pp. 236-238.
- ⁶Hopwood, F. L., "Water Bells," *Proceedings of the Royal Society of London*, Vol. B65, Royal Society of London, London, 1952, pp. 2-5.
- ⁷Lance, G. N., and Perry, R. L., "Water Bells," *Proceedings of the Royal Society of London*, Vol. B66, Royal Society of London, London, 1953, pp. 1067-1072.
- ⁸Taylor, G. I., "The Dynamics of Thin Sheets of Fluid, Part I: Water Bells," *Proceedings of the Royal Society of London*, Vol. A253, Royal Society of London, London, 1959, pp. 289-295.
- ⁹Baird, M. H. I., and Davidson, J. F., "Annular Jets—I. Fluid Dynamics," *Chemical Engineering Science*, Vol. 17, No. 10, 1967, pp. 467-472.
- ¹⁰Hovingh, J., "First Wall Response to Energy Deposition in Conceptual Laser Fusion Reactors," Lawrence Livermore Lab., UCRL-77588, Revision 1, Livermore, CA, May 1977.
- ¹¹Hoffman, M. A., Takahashi, R. K., and Monson, R. D., "Annular Liquid Jet Experiments," *ASME Journal of Fluids Engineering*, Vol. 102, No. 5, 1980, pp. 344-349.
- ¹²Lefebvre, A. H., *Gas Turbine Combustion*, McGraw-Hill, New York, 1983, pp. 371-383.
- ¹³Mongia, H. C., Reynolds, R. S., and Srinivasan, R., "Multidimensional Gas Turbine Combustion Modeling: Application and Limitations," *AIAA Journal*, Vol. 24, No. 6, 1986, pp. 890-904.
- ¹⁴Ferrenberg, A. J., and Varma, M. S., "Atomization Data Requirement for Combustor Modeling," NASA NAS8-34504, June 1986.
- ¹⁵Warsi, Z. U. A., "Conservation Form of the Navier-Stokes Equations in General Nonsteady Coordinates," *AIAA Journal*, Vol. 19, No. 2, 1981, pp. 240-242.
- ¹⁶Zhang, H., Camarero, R., and Kahawita, R., "Conservation Form of the Equations of Fluid Dynamics in General Nonsteady Coordinates," *AIAA Journal*, Vol. 23, No. 11, 1985, pp. 1819, 1820.
- ¹⁷Rizk, N. K., and Lefebvre, A. H., "The Influence of Liquid Film Thickness on Airblast Atomization," *ASME Journal of Engineering for Power*, Vol. 102, No. 7, July 1980, pp. 706-710.
- ¹⁸Levich, V. G., *Physicochemical Hydrodynamics*, Prentice-Hall, Englewood Cliffs, NJ, 1962, pp. 372-380.
- ¹⁹Lefebvre, A. H., *Atomization and Sprays*, Hemisphere, New York, 1989, pp. 173-181.